Acid-Induced Molten Globule State of a Fully Active Mutant of Human Interleukin-6[†]

Vincenzo De Filippis, Patrizia Polverino de Laureto, Nicoletta Toniutti, and Angelo Fontana*

CRIBI Biotechnology Centre, University of Padua, Via Trieste 75, 35121 Padua, Italy

Received February 26, 1996; Revised Manuscript Received April 23, 1996[⊗]

ABSTRACT: Interleukin-6 (IL-6), a four-helix bundle protein, is a multifunctional cytokine which plays an important role in the regulation of the immune system, hematopoiesis, and inflammatory response, as well as in the pathogenesis of multiple myeloma. We have previously shown that a single-disulfide variant of human IL-6, lacking 22 N-terminal amino acids and the disulfide bond connecting Cys-45 and Cys-51 in the 185-residue chain of the wild-type protein, fully retains the conformational, stability, and functional properties of the full-length human IL-6 [Breton et al. (1995) *Eur. J. Biochem. 227*, 573−581]. In this study, we have investigated the conformational and stability properties of mutant IL-6 at acidic pH (A-state). Using far- and near-ultraviolet (UV) circular dichroism (CD), fluorescence emission, and second-derivative absorption spectroscopy, we have established that mutant IL-6 at pH 2.0 fully retains the helical secondary structure of the native protein at pH 7.5, while the tertiary interactions are much weaker. At variance from the native species, mutant IL-6 in the A-state binds 1-anilinonaphthalene-8-sulfonic acid (ANS), a property considered most typical of a protein in the molten globule state. The pH-induced conformational change from the native to the A-state, monitored either by near-UV CD or by ANS-binding measurements, shows a transition midpoint at pH ∼4.5, thus indicating that the partial unfolding of the protein is mediated by the titration of glutamic and/or aspartic acid residues. At pH 2.0, the thermal denaturation of mutant IL-6 occurs as a broad process of low cooperativity with a transition at 50−60 °C, whereas at pH 7.5 the thermal unfolding is cooperative and characterized by a transition midpoint at 65 °C. Of interest, the unfolding of the A-state is not complete even up to ∼85 °C. The urea-mediated unfolding profile of mutant IL-6, measured by far-UV CD, is essentially identical at both pH 7.5 and 2.0, with a midpoint of the cooperative unfolding transition at 5.5 ± 0.1 M denaturant. Both thermal and urea denaturations of the A-state are complex and cannot fit to a two-state model for unfolding. The unusual stability of mutant IL-6 in acid is also reflected by the resistance to proteolysis at pH 3.6−4.0 by *Staphylococcus aureus* V8 protease or cathepsin D, an acid protease released by machrophages upon inflammatory stimulation. It is suggested that the molten globule state of IL-6 at acidic pH can play a role in the biological activity of this cytokine, which can exert its activity also at mildly acidic pH, as in inflammation sites.

The recent and strong interest in partly folded states of proteins, usually denoted molten globules, resides in the fact that these can be used as experimental model systems to unravel the principles underlying protein folding and stability (Ptitsyn, 1995a,b; Dobson, 1992, 1994). Moreover, molten globules can play a role in several physiologically relevant processes and genetic diseases (Ptitsyn, 1995a; Thomas et al., 1995). There is evidence that these partly folded states are those sampled by an unfolded polypeptide chain during the folding process prior to the appearance of the native structure (Ptitsyn et al., 1990; Jennings et al., 1993; Balbach et al., 1995). The early formation of these intermediates leads to a dramatic reduction of the conformational space to be searched during protein folding, and thus an understanding of the mechanisms of formation and stability of these states could considerably simplify the protein folding problem (Kim & Baldwin, 1990; Peng & Kim, 1994; Dobson, 1994). There have been numerous reports describing the structural features of partly folded states of proteins generated by alteration of their amino acid sequence, by removal of protein-bound ligands or prosthetic groups, or by variation of solvent conditions [see Ptitsyn (1995a) for a review]. Consensus characteristics of molten globules include a considerable amount of native-like secondary structure, a compact fold lacking well-defined tertiary interactions, enhanced surface accessibility to solvent, and low cooperativity of thermal unfolding (Kuwajima, 1989; Haynie & Freire, 1993; Dobson, 1994; Peng & Kim, 1994; Ptitsyn, 1992, 1995a).

In this report, we characterize the partly folded state of a single-disulfide form of human interleukin-6 (IL-6)[1] at low pH. This multifunctional cytokine is produced by a wide variety of cells and is involved in the regulation of immune system, hematopoiesis, and inflammatory response (Kishimoto & Hirano, 1988). IL-6 displays its function by

[†] This work was supported in part by Pharmacia-Farmitalia (Milan, Italy).

* To whom correspondence should be addressed [Phone (+39)-49-827-6156; FAX (+39)-49-827-6159].

[⊗] Abstract published in *Advance ACS Abstracts,* August 1, 1996.

[1] Abbreviations: ANS, 1-anilinonaphthalene-8-sulfonic acid; UV, ultraviolet; CD, circular dichroism; [θ], mean residue ellipticity; TFA, trifluoroacetic acid; Tris, tris(hydroxymethyl)aminomethane; Gdn·HCl, guanidine hydrochloride; IL-6, interleukin-6; mutant IL-6, recombinant human des-(A1-S22)-[C45S,C51S]IL-6 with a deletion of 22 amino acid residues at its N-terminus and with a Cys → Ser substitution at positions 45 and 51 of the wild-type polypeptide chain; N- and A-states, folded form of mutant IL-6 at neutral and acidic pH, respectively.

S0006-2960(96)00458-8 CCC: $12.00

inducing terminal differentiation in B lymphocytes and by activating T cells and macrophages (van Snick, 1990). Dysregulation of IL-6 production has been associated with autoimmune diseases such as rheumatoid arthritis and with a number of malignancies such as multiple myeloma and leukemia [see Savino et al. (1994) for references]. Some of these activities are shared by other cytokines, including leukemia inhibitory factor, oncostatin M, ciliary neurotrophic factor, and interleukins-2, -4, and -11. These cytokines are structurally and functionally related, since they show a common four α-helical bundle structure and a similar signal transduction pathway (Paonessa et al., 1995). In a recent study (Nishimura et al., 1996), the overall folding of human IL-6 has been determined by NMR measurements, and the four helical segments were shown to be arranged in an up-up-down-down topology, in agreement with the prediction previously advanced by Bazan (1991). The structural features of IL-6 were found quite similar to those of granulocyte colony-stimulating factor. The X-ray structure of this factor (Lovejoy et al., 1993) was previously utilized for deriving a 3D model of human IL-6 (Savino et al., 1994). IL-6 from various sources, as well as several IL-6 mutants, has been the subject of spectroscopic studies in order to gain insights into structure-stability-function relationships of this cytokine (Breton et al., 1995; Rock et al., 1994; Ward et al., 1993; Hammacher et al., 1994). More recently, a detailed study on the equilibrium denaturation of recombinant murine IL-6 has been reported by Simpson and co-workers (Ward et al., 1995).

The mutant form of human IL-6 we have studied here lacks 22 N-terminal amino acid residues and presents a Cys → Ser substitution at positions 45 and 51, that are connected by a disulfide bond in the wild-type polypeptide chain (Figure 1). In a previous study (Breton et al., 1995), a detailed chemical, physicochemical, and functional characterization of mutant IL-6, conducted at neutral pH, allowed us to firmly establish that this species fully retains the conformational, stability, and functional properties of the recombinant wild-type protein. Therefore, the results obtained here on mutant IL-6 can be extended to the full-length wild-type protein. Our findings indicate that at low pH mutant IL-6 has characteristics of a molten globule (Ptitsyn, 1995a), possessing a native-like fold rather stable toward thermal and urea-induced denaturation, as well as resistant to proteolytic degradation. The possible biological significance of the acid-induced molten globule state of IL-6 is also discussed.

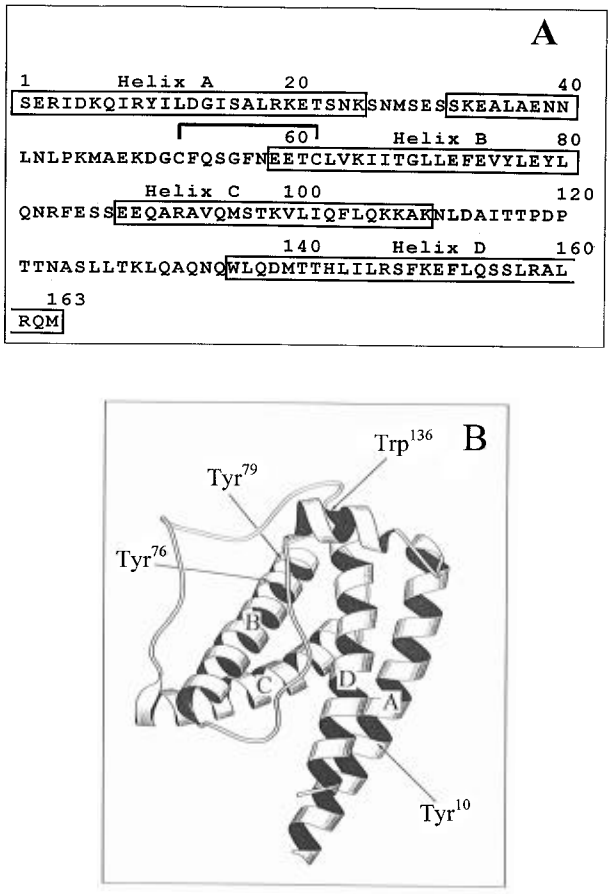

FIGURE 1: Amino acid sequence (A) and schematic representation of the 3D structure (B) of mutant IL-6. Amino acid residues are given in the one-letter code, and residues predicted in α-helical segments are boxed. The location of the single disulfide bond between Cys-52 and Cys-62 is shown by a solid line. The model (B) was obtained as described under Materials and Methods, and the ribbon drawing was generated by using the program MOLSCRIPT (Kraulis, 1991).

MATERIALS AND METHODS

Materials

Purified mutant IL-6 was kindly provided by the Department of Biotechnology, Pharmacia-Farmitalia (Milan, Italy). The Glu-C endoprotease from *Staphylococcus aureus* V8 and horse myoglobin were purchased from Sigma (St. Louis, MO) and bovine spleen cathepsin D from Fluka (Buchs, Switzerland). Trifluoroacetic acid (TFA) and 1-anilinonaphthalene-8-sulfonic acid (ANS) were obtained from Fluka, while other reagent-grade chemicals were from Merck (Darmstadt, Germany).

Methods

Ultraviolet Absorption. Protein concentration was determined by absorption measurements at 280 nm on a double-beam Model Lambda-2 spectrophotometer from Perkin-Elmer (Norwalk, CT). Extinction coefficients at 280 nm for mutant IL-6 and myoglobin were calculated according to Gill and von Hippel (1989) and taken as 0.51 and 1.79 $mg^{-1}\cdot cm^2$, respectively.

Second-derivative ultraviolet absorption spectra of mutant IL-6 (100−150 μg) in 300 μL of buffer were taken at 25 °C after 30 min incubation. The average exposure of tyrosine residues to solvent (α) in different experimental conditions was calculated according to Ragone et al. (1984). A model-compound solution having the same Tyr/Trp molar ratio (3:1) as that found in the mutant IL-6 was employed. Spectra were taken with mutant IL-6 dissolved in 10 mM Tris·HCl−0.1 M NaCl, pH 7.5, or in 10^{-2} M HCl−0.1 M NaCl, pH 2.0. The unfolded state of mutant IL-6 was obtained in the presence of 6 M Gdn·HCl at pH 2.0.

Circular Dichroism. Circular dichroism (CD) spectra were recorded on a Jasco (Tokyo, Japan) Model J-710 spectropolarimeter equipped with a thermostated cell-holder and a NesLab (Newington, NH) Model RTE-110 water circulating bath. The instrument was calibrated with *d*-(+)10-camphorsulfonic acid (Toumadje et al., 1992). Far- and near-UV CD spectra were recorded at 25 °C at a protein concentration ranging from 5 to 50 μM, using 0.1 or 1 cm path length quartz cells in the far- and near-UV region, respectively. The results were expressed as mean residue ellipticity, $[\theta]_{MRW}$

$= (\theta_{obs}/10)(MRW/lc)$, where θ_{obs} is the observed ellipticity at a given wavelength, MRW is the mean residue weight of mutant IL-6 taken as 115 Da, l is the cuvette path length in centimeters, and c is the protein concentration in gram per milliliter. The pH-dependence of the CD signal at 222 and 278 nm was determined by adding, under stirring, aliquots (2−10 μL) of 1 M HCl to a solution (1.2 mL) of mutant IL-6 in 5 mM citrate/borate/phosphate buffer, pH 7.5, containing 0.1 M NaCl. Far-UV CD spectra were analyzed in order to estimate the percentage of protein secondary structure using the equation: $\%_{helix} = 100/\{1 + [(\theta_{222nm,obs} - \theta_{222nm,H})/(\theta_{222nm,C} - \theta_{222nm,obs})]\}$, where $\theta_{222nm,obs}$ is the observed mean residue ellipticity at 222 nm and $\theta_{222nm,H}$ and $\theta_{222nm,C}$ are the mean residue ellipticity values for the 100% helical and coil conformation, respectively. Figures for $\theta_{222nm,H}$ and $\theta_{222nm,C}$ at 25 °C were taken as −33 500 and −485 deg·cm^2·dmol^{-1}, respectively, according to Scholtz et al. (1991).

Fluorescence. Fluorescence emission spectra were recorded at 25 °C on a Perkin-Elmer spectrofluorimeter Model LS-50B, exciting the samples (∼10 μM) at 280 nm and recording the emission fluorescence in the wavelength range 285−500 nm. The binding of ANS to mutant IL-6 was measured by adding 50 μL of ANS stock solution (100 μM) to 450 μL of protein dissolved (2 μM) in buffer (ANS/protein molar ratio 5:1). After 2 h incubation, samples were excited at 390 nm, and the emission fluorescence was recorded in the wavelength range 400−700 nm. The binding of ANS to mutant IL-6 in the pH range 2−8 was followed by measuring the ANS fluorescence signal at λ_{max} as a function of pH. Aliquots (2−30 μL) of 1 N HCl were added to a solution (3 mL) of mutant IL-6 (2 μM) incubated for 1 h with a 20-fold molar eccess of ANS in 5 mM citrate/borate/phosphate buffer, pH 7.5−0.1 M NaCl. The concentration of ANS was determined spectrophotometrically using an extinction coefficient of 5000 cm^{-1}·M^{-1} at 350 nm (Weber & Young, 1964).

Gel Filtration Chromatography. Analytical gel filtration chromatography was carried out loading samples (50 μL) of mutant IL-6 (0.1 mg/mL) onto a Superose-12 column (1 × 30 cm) (Pharmacia, Uppsala, Sweden) equilibrated with 10 mM Tris·HCl−0.1 M NaCl, pH 7.5, or with 10^{-2} M HCl−0.1 M NaCl, pH 2.0. The column was eluted at a flow rate of 0.3 mL/min, and the absorbance of the effluent was recorded at 226 nm. The column was calibrated using the protein mixture kit of low molecular mass (Pharmacia), according to the method of Corbett and Roche (1984).

Stability Measurements. Heat-induced unfolding of mutant IL-6 was followed by recording the decrease of the CD signal at 222 or 278 nm as a function of the sample temperature. The protein concentration in a 1 cm cuvette was 1 and 50 μM in the far- and near-UV region, respectively, and the heating rate (under stirring) was 50 °C/h. Both CD signal and temperature data were recorded simultaneously by a computer program provided by Jasco. Reversibility of the thermal unfolding process was determined by measuring the recovery of the CD signal at 222 nm upon cooling to 20 °C.

Urea-mediated denaturation curves of mutant IL-6 were determined at 25 °C by measuring the CD signal at 222 and 278 nm. Solutions at different urea concentrations were prepared by diluting with buffer a 10 M urea stock solution dissolved in 10 mM Tris·HCl−0.1 M NaCl, pH 7.5, or 10^{-2} M HCl−0.1 M NaCl, pH 2.0. Samples (100 μL) of mutant IL-6 (20 μM) were added to 900 μL of urea solution at the appropriate concentration and incubated at room temperature for 2 h prior to CD measurements. Reversibility of the unfolding process was determined by 10-fold dilution with buffer of protein samples denatured in 9 M urea and measuring the recovery of the ellipticity at 222 nm.

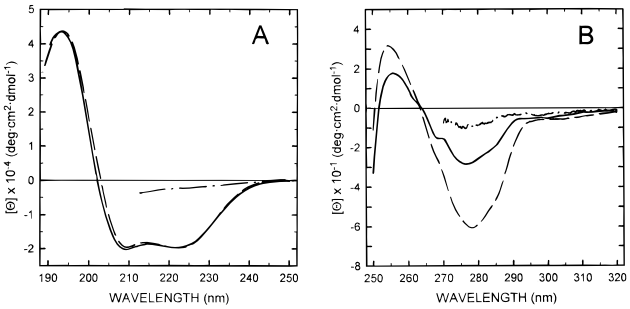

FIGURE 2: Far- (A) and near-UV (B) CD spectra of mutant IL-6. Spectra were taken at 25 °C in 10 mM Tris·HCl−0.1 M NaCl, pH 7.5 (− −), 10^{-2} M HCl−0.1 M NaCl, pH 2.0 (—), or 6 M Gdn·HCl in Tris buffer (− · −).

Proteolysis Experiments. Mutant IL-6 (0.9 mg/mL) was subjected to proteolysis with Glu-C protease from *Staphylococcus aureus* V8 (Drapeau, 1977) at a protease/substrate ratio of 1:50 (by mass) in 50 mM ammonium acetate, pH 4.0, or with cathepsin D from bovine spleen (Fruton, 1987) at a protease/substrate ratio of 1:50 or 1:180 (by mass) in 10 mM sodium citrate buffer, pH 3.6. The reaction mixture was incubated at 37 °C for 2 h, and proteolysis was stopped by diluting an aliquot of the digestion mixture (50 μL) with an equal volume of 1% (v/v) aqueous TFA. Samples were loaded onto a Vydac C4 column (4.6 × 150 mm) equilibrated with 0.05% (v/v) aqueous TFA and eluted with a linear acetonitrile−0.05% TFA gradient from 5 to 30% in 4 min and from 30 to 54% in 18 min, at a flow rate of 0.6 mL/min. The absorbance of the effluent at 226 nm was recorded. The percent recovery of intact protein was determined by integrating the area under the HPLC peak of the protein. For comparison, enzymatic digestions and analyses were also conducted on apomyoglobin under identical experimental conditions. Apomyoglobin was obtained by acetone/HCl precipitation of horse myoglobin (Rossi Fanelli et al., 1958).

Model Building. The structure of mutant IL-6 was modeled on the 1.7 Å X-ray structure of bovine granulocyte-colony stimulating factor (bG-CSF), deposited in the Brookhaven Data Bank as 1BGD (Lovejoy et al., 1993), and on the NMR structure of recombinant human CSF, deposited as 1GNC (Zink et al., 1994). The model was built following the procedure previously reported by Savino et al. (1994) using the homology modeling option included in the program WHAT IF (Vriend, 1990), run on a Silicon Graphics IRIS SD/35 workstation. Amino acid side-chains were positioned using the side-chain rotamer option implemented in WHAT IF (De Filippis et al., 1994), and the refinement of the model structure was achieved by energy-minimization (Brunger, 1990).

RESULTS

Conformational Analysis. (a) Circular Dichroism. Far-ultraviolet CD spectra reported in Figure 2A indicate that, even at pH 2.0 (A-state), mutant IL-6 fully retains the secondary structure content of the protein at neutral pH. The far-UV CD spectrum is typical of α-helical polypeptides with

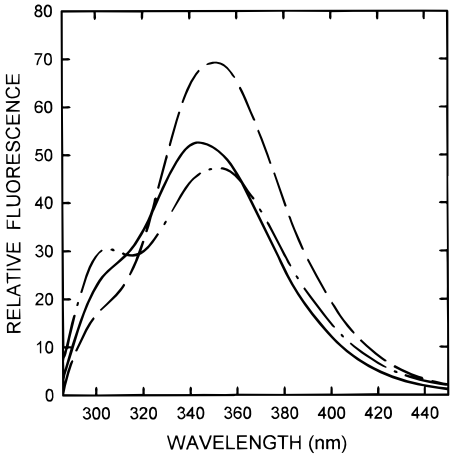

FIGURE 3: Fluorescence emission spectra of mutant IL-6. Spectra were taken, exciting the samples (10 μM) at 280 nm and 25 °C in 10 mM Tris·HCl−0.1 M NaCl, pH 7.5 (− −), 10^{-2} M HCl−0.1 M NaCl, pH 2.0 (—), or 6 M Gdn·HCl in Tris buffer (− · −).

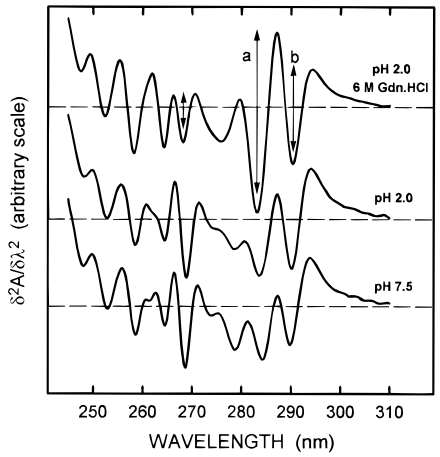

FIGURE 4: Second-derivative ultraviolet absorption spectra of mutant IL-6. Spectra were taken at 25 °C in 10 mM Tris·HCl−0.1 M NaCl, pH 7.5, 10^{-2} M HCl−0.1 M NaCl, pH 2.0, or 6 M Gdn·HCl in Tris buffer. Dashed lines indicate where the value of $d^2A/d\lambda^2$ is zero. The peak-to-through distance between the maximum at 287 nm and minimum at 283 nm (a) and that between the maximum at 295 nm and the minimum at 290.5 nm (b) were used to calculate the Tyr exposure according to Ragone et al. (1984). The peak-to-through distance between the maximum at 266 nm and the minimum at 268 nm, due to the contribution of Phe residues, is also indicated.

ellipticity minima at 208 and 222 nm. Quantitative analysis of CD spectra allowed us to estimate as 59% the α-helical content of mutant IL-6 (see Materials and Methods). This value is in full agreement with that obtained from the proposed model structure of the protein, which accounts for 61% α-helix (Savino et al., 1994) (see Figure 1). The CD signal in the near-UV region at pH 2.0 is significantly lower (∼50%) than that measured at pH 7.5 (Figure 2B), suggesting that the addition of acid induces a looser and more flexible environment nearby aromatic residues (Strickland, 1974). Nevertheless, the overall features of the near-UV CD spectrum and, in particular, the presence of a fine structure in the 258−270 nm region, associated with phenylalanine residues (Strickland, 1974), suggest that tertiary interactions do exist in the protein in its A-state. On the other hand, in the presence of the strong protein denaturant 6 M Gdn·HCl, mutant IL-6 loses its secondary and tertiary structure, as given by the far- and near-UV CD spectra (Figure 2).

(b) Fluorescence Emission. The fluorescence spectrum of mutant IL-6 taken at pH 7.5 shows a maximum of emission at 351 nm, which indicates that the single Trp-136 of the protein is fully exposed to solvent (Lakowicz, 1986). The spectrum of the protein at pH 2.0 shows a reduced Trp fluorescence intensity, a blue-shift of λ_{max} to ∼340 nm, and an increased contribution of Tyr fluorescence at ∼303 nm (Figure 3). The enhanced Tyr fluorescence may arise from a weakening of the Tyr-to-Trp energy transfer in the more relaxed structure of mutant IL-6 at low pH. Measurements conducted on model compounds show that, on going from neutral to acidic pH, the tryptophanyl quantum yield is reduced, while λ_{max} remains constant (not shown). This suggests that the reduction of the Trp emission observed for mutant IL-6 at pH 2.0 is primarily caused by an acid quenching of fluorescence, while the shift of λ_{max} to shorter wavelengths may arise from changes in the polarity of the microenvironment near the single Trp residue (Lakowicz, 1986). Analytical gel filtration chromatography of mutant IL-6, conducted at pH 2.0 (see Materials and Methods), allowed us to exclude the presence of aggregates that, otherwise, could have led to the burial of Trp-136, with a consequent blue-shift of λ_{max} of the fluorescence emission. The fluorescence data (Figure 3) can be interpreted by considering that Trp-136 is at the protein surface in the proposed model, located at the beginning of helix D (Savino et al., 1994) (see Figure 1), followed by Asp-139 at the $i+3$ position in the polypeptide chain. At low pH, the carboxylate group of the aspartyl side chain becomes uncharged, causing a less polar environment near the Trp-136 residue and thus a blue-shift of the Trp fluorescence (Lakowicz, 1986).

(c) Second-Derivative Absorption. This spectroscopic technique can be used to estimate the solvent exposure of Tyr residues in proteins, taking advantage of the fact that peak-to-through distances in the 280−295 nm region, expressed as *a/b* ratio (see Figure 4), are related to the polarity of the medium in which Tyr residues are embedded (Ragone et al., 1984). Moreover, it has been shown that an increase in water accessibility of Phe residues is associated with a decrease in the 266−268 nm peak-to-through distance (Ichikawa & Terada, 1979; Pfeil, 1993). Second-derivative spectra of mutant IL-6 recorded at pH 7.5 and pH 2.0 share common features (Figure 4), but some differences are seen in the 280−295 nm region. We have previously calculated from second-derivative spectra (Breton et al., 1995) ∼$^1/_3$ average exposure of the three Tyr residues in mutant IL-6 at neutral pH, in agreement with the results of NMR studies conducted on the full-length human IL-6 (Nishimura et al., 1990) and with the proposed model structure (Savino et al., 1994; see Figure 1). In fact, Tyr-10 in mutant IL-6 is located in helix A and on the protein surface, while the other two Tyr residues (Tyr-76 and Tyr-79) are located in helix B and shielded from the solvent by the long loop connecting helices C and D (see Figure 1). Analysis of the spectra shown in Figure 4 gave a ∼30% enhanced exposure of Tyr residues of mutant IL-6 in its A-state with respect to that in the N-state. On the other hand, the features of the second-derivative spectrum in the 280−295 nm region of the fully unfolded mutant IL-6 in 6 M Gdn·HCl are much different from those of the protein at pH 7.5 or 2.0. Moreover, the 266−268 nm peak-to-through distance measured at pH 2.0 is only ∼10% lower than that measured at pH 7.5, indicating that the microenvironment near the seven Phe residues is not appreciably altered upon acidification.

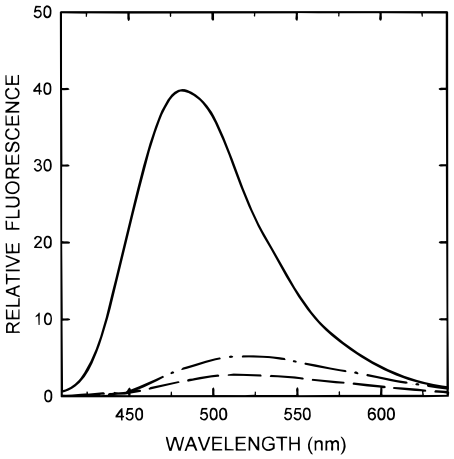

FIGURE 5: Binding of ANS to mutant IL-6. Fluorescence emission spectra of ANS (10 μM) were taken, exciting the sample at 390 nm after 2 h incubation at 25 °C with mutant IL-6 (2 μM) in 10^{-2} M HCl−0.1 M NaCl, pH 2.0 (—), containing 6 M Gdn·HCl (— · —), or in 10 mM Tris·HCl−0.1 M NaCl, pH 7.5 (— —).

(d) ANS Binding. The binding of the hydrophobic dye ANS is a widely used tool to identify and characterize partly folded states of proteins, including molten globules [see Ptitsyn (1992) for references]. ANS binds to hydrophobic regions of proteins with a dramatic increase of the fluorescence quantum yield and with a blue-shift of λ_{max}, reflecting the burial of the ANS molecule in a more hydrophobic environment. As shown in Figure 5, the fluorescence intensity of ANS in the presence of mutant IL-6 at pH 2.0 is much higher than that observed at pH 7.5 or with the fully unfolded protein in the presence of 6 M Gdn·HCl. Moreover, at acidic pH, the λ_{max} of the ANS fluorescence emission is shifted from 520 nm to about 480 nm. These fluorescence data clearly indicate that ANS binds to mutant IL-6 in its A-state only, suggesting that a hydrophobic region becomes exposed to solvent at low pH.

In order to establish a possible correlation between the partial unfolding of mutant IL-6 and the concomitant exposure of hydrophobic groups, the CD signal in the far- and near-UV region (Figure 6A) and also the ANS fluorescence at λ_{max} (Figure 6B) were recorded as a function of pH. The ellipticity value at 222 nm is rather constant over a wide pH range (Figure 6A). At variance, both the ellipticity at 278 nm and the ANS fluorescence intensity at λ_{max} show a sigmoidal pH dependence, with a transition midpoint at pH 4.5 ± 0.1 in both cases. These data suggest that acidification induces a looser side-chain packing in mutant IL-6, as reflected by the reduction of the ellipticity at 278 nm, leading to the exposure to solvent of hydrophobic patches amenable to interact with ANS. This view is supported by the linear correlation of the enhancement of ANS fluorescence intensity with the decrease of the CD signal at 278 nm in the pH range 3−6 (Figure 6C).

Stability Studies. (a) Thermal Unfolding. The heat-induced denaturations of mutant IL-6 at pH 7.5 and 2.0 were studied by monitoring the CD signal at 222 nm, which is a sensitive parameter of the helical secondary structure. The melting profiles for the N- and A-states of mutant IL-6 are shown in Figure 7. At pH 7.5, the unfolding transition was highly cooperative, but irreversible, since the protein partly precipitates from solution when kept at temperatures above ~70 °C. At variance, the thermal denaturation of mutant IL-6 at pH 2.0 was highly reversible (~90%), but poorly cooperative. The A-state of the protein shows a broad, but distinct thermal transition at 50−60 °C (see Figure 7). Of interest, the thermally unfolded state at pH 2.0 still shows significant residual secondary structure, since the $[\theta]_{222nm}$ value decreases from −20 000 ± 500 at 20 °C to −9000 ± 200 deg·cm^2·dmol^{-1} at 85 °C and the far-UV CD spectrum at pH 2.0 of mutant IL-6 recorded at 85 °C still shows features typical of helical polypeptides (not shown). The figure of $[\theta]_{222nm}$ extrapolated at 110 °C is ~−5000 deg·cm^2·dmol^{-1}, which is characteristic for all denatured globular proteins at this temperature (Griko et al., 1994).

The heat denaturation of the A-state of mutant IL-6 was also monitored by recording the temperature dependence of $[\theta]_{278nm}$, which is associated with the asymmetric environment within the protein matrix of Tyr residue(s) (Strickland, 1974) and thus serves as a probe of tertiary structure. The data of Figure 7 clearly show that the tertiary structure of the A-state of mutant IL-6 is much more heat-labile than its secondary structure. The CD signal at 278 nm sharply decreases at temperatures above 20 °C, while the unfolding of the tertiary structure appears to be complete at ~60 °C. The near-UV CD spectrum at 60 °C of mutant IL-6 at pH 2.0 is essentially absent (not shown) and similar to that measured for the fully unfolded protein in 6 M Gdn·HCl (see Figure 2B).

(b) Unfolding by Urea. To further characterize the stability properties of mutant IL-6 in the A-state with respect to those in the N-state, we compared the urea-induced unfolding transitions of the protein at pH 2.0 and 7.5. As shown in Figure 8, the profiles of $[\theta]_{222nm}$ *versus* urea concentration of mutant IL-6 in both the N- and A-states are essentially identical. The concentration of denaturant at which the protein is half-unfolded is 5.5 ± 0.1 M in both cases. Moreover, the urea-mediated unfolding transitions were highly cooperative and completely reversible (>95%) at both neutral and acidic pH. On the other hand, when the unfolding transition of the A-state was monitored by measuring $[\theta]_{278nm}$ *versus* urea concentration, *i.e.*, by monitoring the unfolding of the tertiary structure of the protein (see above), it was found that the tertiary interactions in the A-state are highly labile to urea denaturation and that the loss of tertiary structure significantly precedes that of the secondary structure of the protein (see Figure 8).

(c) Proteolysis. Among its numerous physiological activities, IL-6 plays a key role in inflammatory processes (van Snick, 1990). The extracellular space of inflammatory sites is characterized by a low pH, and near the surface of activated macrophages, the pH is as low as 3.6 (Silver et al., 1988), while several proteases of different substrate specificities are also present (see Discussion). It is conceivable to suggest that IL-6, in order to exploit its biological function, should retain a sufficiently stable conformation in these environments. In order to test this hypothesis, we incubated mutant IL-6 at pH 4.0 with the Glu-C protease from *Staphylococcus aureus* V8 (Drapeau, 1977) and at pH 3.6 with cathepsin D (Fruton, 1987), an endogenous acid protease fully active at this pH and released by macrophages in response to inflammatory stimulation. For comparative purposes, proteolysis experiments were also conducted, under identical experimental conditions, on horse apomyoglobin, which in acid solution maintains approximately half of the secondary structure content of the protein at neutral pH (Goto

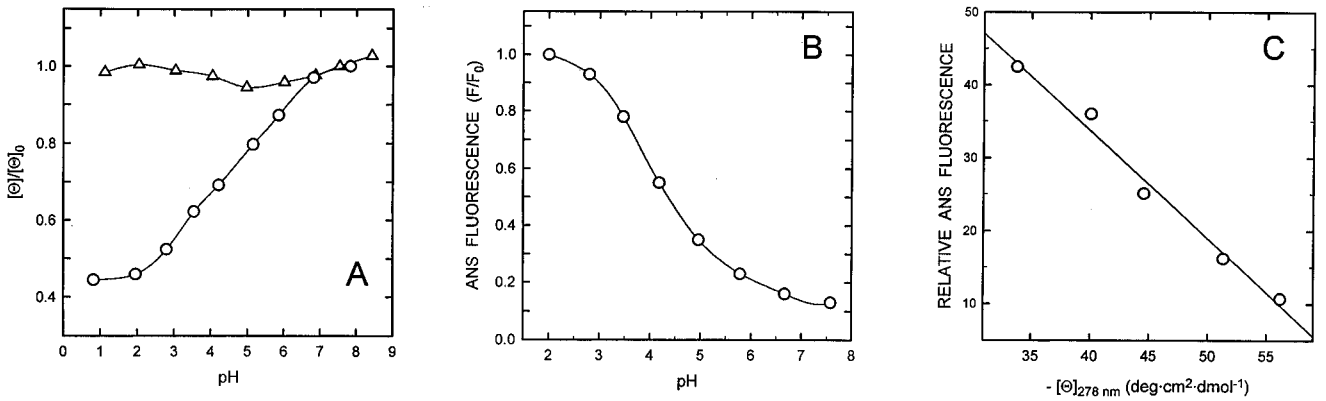

FIGURE 6: (A) pH dependence of the far- and near-UV CD signal of mutant IL-6. The CD signal at 222 (△) or 278 nm (○) of mutant IL-6 was taken at 25 °C in a 1-cm cuvette at protein concentrations of 1 and 50 μM in the far- and near-UV region, respectively, in 5 mM citrate/borate/phosphate buffer at the indicated pH. Ellipticity data are given as the $[\theta]/[\theta]_o$ ratio, where $[\theta]_o$ is the ellipticity value measured at pH 7.5. (B) pH dependence of the binding of ANS to mutant IL-6. The protein (2 μM) was incubated for 1 h with a 20-fold molar excess of ANS at pH 7.5 (see Materials and Methods). The fluorescence of ANS at each pH was taken after exciting the sample at 390 nm and recording the fluorescence intensity at λ_{max}. Data are given as the F/F_o ratio, where F_o is the fluorescence signal recorded at pH 2.0. (C) Correlation between ANS fluorescence at λ_{max} and $[\theta]_{278nm}$ of mutant IL-6. ANS fluorescence emission data (panel B) are plotted *versus* the near-UV CD signal at 278 nm (panel A) in the pH range 3−6.

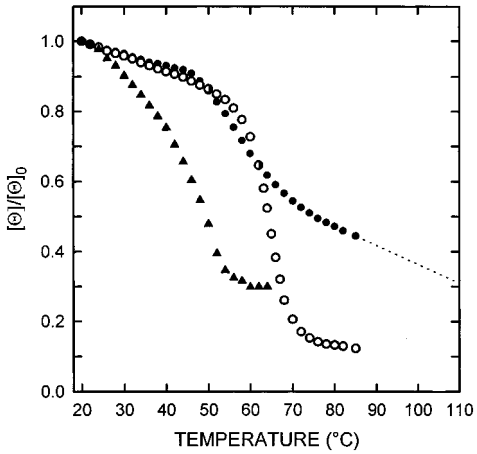

FIGURE 7: Heat-induced denaturation of mutant IL-6. The thermal unfolding was followed by monitoring the CD signal at 222 nm in 10 mM sodium phosphate−0.1 M NaCl, pH 7.5 (○), or in 10^{-2} M HCl−0.1 M NaCl, pH 2.0 at 222 nm (●) or 278 nm (▲). Data are given as the $[\theta]/[\theta]_o$ ratio, where $[\theta]_o$ is the ellipticity value measured at 20 °C. The dotted line indicates the linear extrapolation of $[\theta]_{222nm}$ to 110 °C.

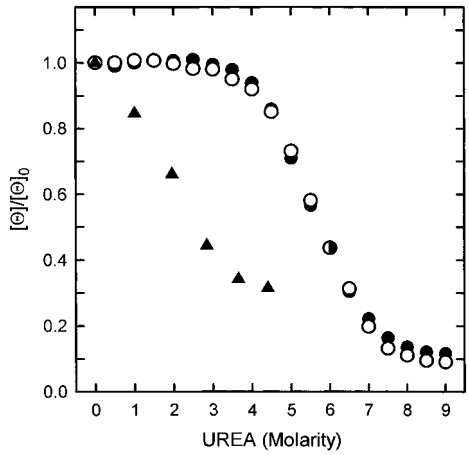

FIGURE 8: Urea-induced unfolding of mutant IL-6. Measurements were carried out at 25 °C in 10 mM Tris·HCl−0.1 M NaCl, pH 7.5 (○), or in 10^{-2} M HCl−0.1 M NaCl, pH 2.0 at 222 (●) and 278 nm (▲). Data are given as the $[\theta]/[\theta]_o$ ratio, where $[\theta]_o$ is the ellipticity value measured in the absence of denaturant.

& Fink, 1990). The results shown in Figure 9 clearly indicate that, after 2 h incubation at 37 °C, mutant IL-6 is rather resistant to proteolytic digestion by both V8 protease and cathepsin D, while apomyoglobin is almost fully degraded. Assuming that the experimental conditions of proteolysis herewith employed mimic to some extent those experienced by IL-6 *in vivo*, it is conceivable to suggest that IL-6 could display its biological activity even in the A-state, which is acid-stable and rather resistant to proteolytic attack.

DISCUSSION

The A-State of Mutant IL-6. The results of this study indicate that the four-helix bundle protein mutant IL-6 at low pH retains the secondary structure elements of the native species at neutral pH, while an acid-mediated partial unfolding of the protein leads to a weakening of tertiary interactions and an enhanced solvent exposure of hydrophobic groups. However, the reduced (∼50%) but still significant near-UV CD signal of mutant IL-6 in its A-state does not imply global disorder of the protein molecule, but may reflect local perturbations of the tertiary structure, *e.g.*, nearby Tyr residues, which are the major contributors of the near-UV CD spectrum of mutant IL-6 [Strickland, 1974; see also Breton et al. (1995)]. Although present data alone do not allow a detailed picture of the structural features of the A-state, they provide useful information on the N ⇔ A conformational transition. In particular, the pH dependence of both near-UV CD and ANS binding (Figure 6) indicates that the partial unfolding of mutant IL-6 in acid occurs with a transition midpoint at pH ∼4.5 ± 0.1, thus indicating that the conformational change is mediated by the titration of Glu and/or Asp residue(s). It can be proposed that, upon acid titration, intramolecular charge repulsion is the driving force for partial unfolding of the protein molecule, thus inducing a looser side-chain packing and the exposure to solvent of hydrophobic groups (Goto et al., 1990; Fink et al., 1994).

In recent years, several proteins were shown to acquire a partly folded state at acidic pH, commonly called the A-state. It was found that the A-state of proteins is characterized by significant structural variability, so that only general features

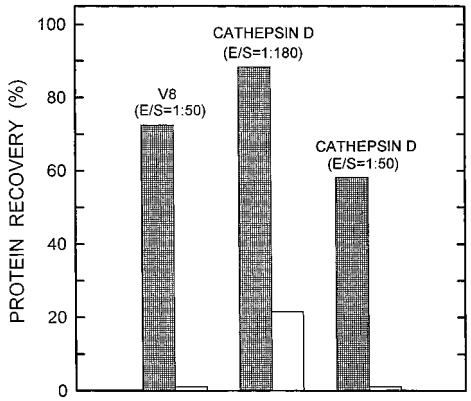

FIGURE 9: Enzymatic digestion of mutant IL-6 and horse apomyoglobin. Proteolysis with *S. aureus* V8 protease was conducted at 37 °C in 50 mM ammonium acetate buffer, pH 4.0, and with cathepsin D in 10 mM sodium citrate buffer, pH 3.6, at the indicated enzyme/substrate (E/S) ratio. The percent recovery of intact protein was determined as described under Materials and Methods. Mutant IL-6, filled bars; horse apomyoglobin, open bars.

of this state can be given [see Fink et al. (1994) and Fink (1995) for references]. The A-state of mutant IL-6 appears to maintain not only a native-like secondary structure but also some specific packing of side-chain groups in the tertiary structure, as given by CD measurements (see Figure 2). Thus, it seems that the conformational features of the A-state of mutant IL-6 can be related to those of the so-called "highly-ordered" molten globules, such as IL-4 (Redfield et al., 1994), apocytochrome b_{562} (Feng et al., 1994), or equine lysozyme (Morozova et al., 1995).

Stability of the A-State. Mutant IL-6 in its A-state shows a noteworthy stability to both heat- and urea-mediated denaturation. Even if the thermal unfolding profile of the A-state monitored by $[\theta]_{222nm}$ is quite broad, a distinct transition is observed at 50−60 °C. Of interest, the A-state even at 85 °C is not fully unfolded, but still maintains significant residual secondary structure (see Figure 7). This has been previously observed also in thermally denatured proteins (Tanford, 1968; Wong & Tanford, 1973), *e.g.*, ribonuclease A (Robertson & Baldwin, 1991) and lysozyme (Evans et al., 1991), and in the heat-induced denaturation of apo-α-lactalbumin molten globule (Griko et al., 1994). It has been proposed that the residual structure of these proteins at high temperature, as well as of the protein molten globules, is stabilized primarily by nonspecific hydrophobic interactions (Griko et al., 1994; Khurana & Udgaonkar, 1994) and that thermal denaturation leads to an ensemble of conformations possessing different degrees of residual structure that progressively unfold upon further heating (Freire, 1995). The thermal unfolding profiles, shown in Figure 7, indicate that the secondary structure of mutant IL-6 in its A-state is more stable that its tertiary structure, suggesting that the heat-induced denaturation cannot be regarded as a classical two-state process (Lumry et al., 1966). The higher stability of the secondary structure of mutant IL-6 in the A-state may result from the general properties of molten globule states, characterized by secondary structure elements that are stable even in the absence of strong tertiary interactions and that are held together by nonspecific hydrophobic interactions (Kiefhaber & Baldwin, 1995). The sharp decrease of $[\theta]_{278nm}$ that occurs at relatively low temperatures may reflect the fact that the specific tertiary interactions, contributing to the near-UV CD spectrum, are much weaker in the A-state than in the N-state, as given by the reduced intensity of the CD signal at 278 nm (see Figure 2B).

While the melting profile of the A-state is different from that of the N-state (Figure 7), the urea-mediated unfolding, monitored by far-UV CD measurements, is identical for both states and occurs as a highly cooperative and reversible process (midpoint transition at 5.5 ± 0.1 M urea) (Figure 8). Likely, this can be explained by considering that urea denatures proteins mainly by weakening hydrogen bonds of peptide groups within secondary structure elements (Scholtz et al., 1995) and, to a minor extent, by solubilizing nonpolar side-chains (Creighton, 1979). Consequently, since mutant IL-6 maintains the same α-helix content in its A- and N-states, it will similarly interact with urea under neutral and acidic conditions. The different effects of heat and urea on the unfolding of the A-state of mutant IL-6 may arise from the different molecular mechanism by which these two agents denature proteins (Nishii et al., 1995), leading to intrinsically different unfolded states (Dill & Shortle, 1991; Ptitsyn, 1995a). In analogy to the thermal unfolding of mutant IL-6, the tertiary structure of the A-state is much more labile to the denaturing action of urea than its secondary structure (Figure 8). We have previously used urea-induced denaturation data, as given by far-UV CD measurements, to derive the Gibbs free energy of unfolding of mutant IL-6 in its N-state at pH 7.5. Assuming a two-state unfolding process (Pace, 1986), a figure of 20.9 ± 0.4 kJ·mol^{-1} for the thermodynamic stability of the protein at 25 °C in the absence of denaturant was obtained (Breton et al., 1995). On the other hand, the urea-mediated unfolding process of the A-state does not seem to be a two-state process. In fact, a necessary but not sufficient (Dill & Shortle, 1991) condition for such a process is that two (or more) different measured properties (*e.g.*, far- and near-UV CD) should have coincident sigmoidal curves (Lumry et al., 1966). This would imply that the urea-mediated unfolding of the A-state to the fully unfolded state (see Figure 8) is a three-state or multi-state process, as for example previously found for the further unfolding of partly folded states of other proteins (Carra et al., 1994; Barrick & Baldwin, 1993; Freire, 1995). However, in this context it should be mentioned that theoretical studies have indicated that the noncoincidence of the curves of two different physical properties not necessarily disproves a two-state process [see Dill and Shortle (1991) for a discussion].

The actual unfolding of a molten globule state is still debated in current literature (Finkelstein & Shakhnovich, 1989; Shakhnovich & Finkelstein, 1989; Chan & Dill, 1991; Ptitsyn, 1995a; Freire, 1995). A general characteristic commonly attributed to the molten globule includes a low cooperativity for unfolding (Ptitsyn, 1995), or no cooperativity at all (Yutani et al., 1992). Whereas this seems to be true for the thermal unfolding of the A-state of mutant IL-6 when compared to that of the N-state (Figure 7), the urea-mediated unfolding is highly cooperative and identical to that of the N-state (Figure 8). Even if more work is required to shed light on the unfolding process of the A-state of mutant IL-6, the results of this study add weight to the proposal that partly folded intermediates can display cooperative folding/unfolding transitions to a varying degree [Tanford, 1968; Wong & Tanford, 1973; Robson & Pain, 1976; for a recent review, see Freire (1995)]. Thus, it seems that a tight packing might not be a critical prerequisite for the cooperativity of protein unfolding (Xie et al., 1994).

Physiological Role of the A-State. The possible biological significance of the molten globule state of proteins has been recognized recently [Bychkova et al., 1988, 1992; see Ptitsyn (1995a) for references]. It is becoming clear that in order to regulate protein function and turnover in a living cell, molten globule states of proteins can be generated by exposing them to "unusual" denaturing conditions (Ptitsyn, 1995a). In fact, the native-like overall fold of a molten globule, together with its enhanced flexibility, likely can dictate a number of ideal properties for a functional protein in a living cell and could facilitate the insertion into and translocation across membranes, chaperone-mediated protein folding *in vivo*, cell fusion, and protein-receptor interactions (Ptitsyn, 1995a). Of outstanding interest is the possible role of the molten globule in the mechanism of some severe diseases, such as cystic fibrosis (Thomas et al., 1995). Among the various biological activities of IL-6, this cytokine plays a major role in the pathogenesis of inflammation (van Snick, 1990). This environment is characterized by an acidic pH, down to 3.6 near the surface of activated machrophages, and by the presence of a variety of proteolytic enzymes released by machrophages in the extracellular space (Silver et al., 1988). We have shown here that the acid-induced partly folded state of mutant IL-6 is rather stable and also quite resistant to proteolytic degradation. This latter feature of mutant IL-6 in its A-state can be taken as a clear-cut indication of a folded and globular species, since it is well-known that the rigidity of the native structure of a globular protein hampers proteolytic degradation, whereas unfolded, structureless polypeptide chains are fast degraded (Fontana et al., 1993). Thus, IL-6 in inflammation sites likely could acquire a stable and functional molten globule state. This hypothesis appears to be attractive, but more experimental work is required for achieving direct evidence of this proposal.

To summarize, the A-state of mutant IL-6 conforms to the current views of the molten globule state [see Ptitsyn (1995a)], since it displays the helical secondary structure content of the native protein, weaker tertiary interactions, increased exposure of hydrophobic groups, and poor cooperativity of thermal unfolding. On the other hand, the results of this study add weight to the notion that proteins in their molten globule state display structural variability, ranging from highly unfolded (Ptitsyn et al., 1990; Ptitsyn, 1995a) to near native-like structures [Redfield et al., 1994; Feng et al., 1994; see also Miranker and Dobson (1996) for a recent review]. Actually, this variability is causing the current debate on the nature of the molten globule state of proteins (Ewbank et al., 1995; Okazaki et al., 1995).

ACKNOWLEDGMENT

We thank Drs. Gaetano Orsini and Federico Bertolero from Pharmacia-Farmitalia (Milan, Italy) for the generous gift of mutant IL-6. The helpful suggestions of Drs. Gerrit Vriend and Emanuele Papini are also gratefully acknowledged.

REFERENCES

Balbach, J., Forge, V., van Nuland, N. A., Winder, S. L., Hore, P. J., & Dobson, C. M. (1995) *Nat. Struct. Biol. 2*, 865−870.
Barrick, D., & Baldwin, R. L. (1993) *Biochemistry 32*, 3790−3796.
Bazan, J. F. (1991) *Neuron 7*, 197−208.
Breton, J., La Fiura, A., Bertolero, F., Orsini, G., Valsassina, B., Ziliotto, R., De Filippis, V., Polverino de Laureto, P., & Fontana, A. (1995) *Eur. J. Biochem. 227*, 573−581.
Brunger, A. T. (1990) X-PLOR, Manual version 2.1, Yale University, New Haven, CT.
Bychkova, V. E., Pain, R. H., & Ptitsyn, O. B. (1988) *FEBS Lett. 238*, 231−234.
Bychkova, V. E., Berni, R., Rossi, G. L., Kutyshenko, V. P., & Ptitsyn, O. B. (1992) *Biochemistry 31*, 7566−7571.
Carra, J. H., Anderson, E. A., & Privalov, P. L. (1994) *Biochemistry 33*, 10842−10850.
Corbett, R. J. T., & Roche, R. S. (1984) *Biochemistry 23*, 1888−1894.
Creighton, T. E. (1979) *J. Mol. Biol. 129*, 235−264.
De Filippis, V., Sander, C., & Vriend, G. (1994) *Protein Eng. 7*, 1203−1208.
Dill, K. A., & Shortle, D. (1991) *Annu. Rev. Biochem. 60*, 795−825.
Dill, K. A., Bromberg, S., Yue, K., Fiebig, K. M., Yee, D. P., Thomas, P. D., & Chan, H. S. (1995) *Protein Sci. 4*, 561−601.
Dobson, C. M. (1992) *Curr. Opin. Struct. Biol. 2*, 6−12.
Dobson, C. M. (1994) *Curr. Biol. 4*, 636−640.
Drapeau, G. R. (1977) *Methods Enzymol. 47*, 189−191.
Evans, P. A., Topping, K. D., Woolfson, D. N., & Dobson, C. M. (1991) *Proteins: Struct., Funct., Genet. 9*, 248−266.
Ewbank, J. J., Creighton, T. E., Hayer-Hartl, M. K., & Hartl, F. U. (1995) *Nat. Struct. Biol. 2*, 10.
Feng, Y., Sligar, S. G., & Wand, A. J. (1994) *Nat. Struct. Biol. 1*, 30−35.
Fink, A. L. (1995) *Annu. Rev. Biophys. Biomol. Struct. 24*, 495−522.
Fink, A. L., Calciano, L. J., Goto, Y., Kurotsu, T., & Palleros, D. R. (1994) *Biochemistry 33*, 12504−12511.
Finkelstein, A. V., & Shakhnovich, E. I. (1989) *Biopolymers 28*, 1681−1694.
Fontana, A., Polverino de Laureto, P., & De Filippis, V. (1993) in *Stability and Stabilization of Enzymes* (van den Tweel, W. J. J., Harder, A., & Buitelaar, R. M., Eds.) pp 101−110, Elsevier, Amsterdam.
Freire, E. (1995) *Annu. Rev. Biophys. Biomol. Struct. 24*, 141−165.
Fruton, J. S. (1987) in *Hydrolytic Enzymes* (Neuberger, A., & Brocklehurst, K., Eds.) pp 132−145, Elsevier, Amsterdam.
Gill, S. C., & von Hippel, P. H. (1989) *Anal. Biochem. 182*, 319−326.
Goto, Y., & Fink, A. L. (1990) *J. Mol. Biol. 214*, 803−805.
Goto, Y., Takahashi, N., & Fink, A. L. (1990) *Biochemistry 29*, 3486−3488.
Griko, Y. V., Freire, E., & Privalov, P. L. (1994) *Biochemistry 33*, 1889−1899.
Hammacher, A., Ward, L. D., Weinstock, J., Trentlein, H., Yasukawa, K., & Simpson, R. J. (1994) *Protein Sci. 3*, 2280−2293.
Haynie, D. T., & Freire, E. (1993) *Proteins: Struct., Funct., Genet. 16*, 115−140.
Ichikawa, T., & Terada, H. (1979) *Biochim. Biophys. Acta 580*, 120−128.
Jennings, P. A., & Wright, P. E. (1993) *Science 262*, 892−896.
Khurana, R., & Udgaokar, J. B. (1994) *Biochemistry 33*, 106−115.
Kiefhaber, T., & Baldwin, R. L. (1995) *J. Mol. Biol. 252*, 122−132.
Kim, P. S., & Baldwin, R. L. (1990) *Annu. Rev. Biochem. 59*, 631−660.
Kishimoto, T., & Hirano, T. (1988) *Annu. Rev. Immunol. 6*, 485−512.
Kraulis, P. (1991) *J. App. Crystallogr. 24*, 946−950.
Kuwajima, K. (1989) *Proteins: Struct., Funct., Genet. 6*, 87−103.
Lakowicz, J. R. (1986) in *Principles of Fluorescence Spectroscopy* (Lakowicz, J. R., Ed.) pp 341−381, Plenum Press, New York.
Lovejoy, B., Cascio, D., & Eisenberg, D. (1993) *J. Mol. Biol. 234*, 640−653.
Lumry, R., Biltonen, R. L., & Brandts, J. F. (1966) *Biopolymers 4*, 917−945.
Miranker, A. D., & Dobson, C. M. (1996) *Curr. Opin. Struct. Biol. 6*, 31−42.
Morozova, L. A., Haynie, D. T., Arico-Muendel, C., van Dael, H., & Dobson, C. M. (1995) *Nat. Struct. Biol. 2*, 871−875.

Nishii, I., Kataoka, M., & Goto, Y. (1995) *J. Mol. Biol. 250*, 223−238.
Nishimura, C., Hanzawa, H., Itoh, S., Yasukawa, K., Shimada, I., Kishimoto, T., & Arata, Y. (1990) *Biochim. Biophys. Acta 1041*, 243−249.
Nishimura, C., Watanabe, A., Gouda, H., Shimada, I., & Arata, Y. (1996) *Biochemistry 35*, 273−281.
Okazaki, A., Ikura, T., & Kuwajima, K. (1995) *Nat. Struct. Biol.* 2, 10−11.
Pace, C. N. (1986) *Methods Enzymol. 131*, 266−279.
Paonessa, G., Graziani, R., De Serio, A., Savino, R., Ciapponi, L., Salvati, A. L., Toniatti, C., & Ciliberto, G. (1995) *EMBO J. 14*, 1942−1951.
Peng, Z.-Y., & Kim, P. S. (1994) *Biochemistry 33*, 2131−2141.
Pfeil, W. (1993) *Protein Sci. 2*, 1497−1501.
Ptitsyn, O. B. (1992) in *Protein Folding* (Creighton, T. E., Ed.) pp 243−300, W. H. Freeman & Co., New York.
Ptitsyn, O. B. (1995a) *Adv. Protein Chem. 47*, 83−229.
Ptitsyn, O. B. (1995b) *FEBS Lett. 20*, 376−379.
Ptitsyn, O. B., Pain, R. H., Semisotnov, G. V., Zerovnik, R., & Razgulajev, O. I. (1990) *FEBS Lett. 262*, 20−24.
Ragone, R., Colonna, G., Balestrieri, C., Servillo, L., & Irace, G. (1984) *Biochemistry 23*, 1871−1875.
Redfield, C., Smith, R. A. G., & Dobson, C. M. (1994) *Nat. Struct. Biol. 1*, 23−29.
Robertson, A. D., & Baldwin, R. L. (1991) *Biochemistry 30*, 9907−9914.
Robson, B., & Pain, R. H. (1976) *Biochem. J. 155*, 331−334.
Rock, L. R., Li, X., Chong, P., Ida, N., & Klein, M. (1994) *Biochemistry 33*, 5146−5154.
Rossi Fanelli, A., Antonini, E., & Caputo, A. (1958) *Biochim. Biophys. Acta 30*, 608−615.
Savino, R., Lahm, A., Salvati, A. L., Ciapponi, L., Sporeno, E., Altamura, S., Paonessa, G., Toniatti, C., & Ciliberto, G. (1994) *EMBO J. 13*, 1357−1367.
Scholtz, J. M., Qian, H., York, E. J., Stewart, J. M., & Baldwin, R. L. (1991) *Biopolymers 31*, 1463−1470.
Scholtz, J. M., Barrick, D., York, E. J., Stewart, J. M., & Baldwin, R. L. (1995) *Proc. Natl. Acad. Sci. U.S.A. 92*, 185−189.
Shakhnovich, E. I., & Finkelstein, A. V. (1989) *Biopolymers 28*, 1667−1680.
Silver, I. A., Murrils, R. J., & Etherington, D. J. (1988) *Exp. Cell. Res. 175*, 266−267.
Strickland, E. H. (1974) *CRC Crit. Rev. Biochem. 3*, 113−175.
Tanford, C. (1968) *Adv. Protein Chem. 23*, 121−282.
Thomas, P. J., Qu, B.-H., & Pedersen, P. L. (1995) *Trends Biol. Sci. 20*, 456−459.
Toumadje, A., Alcorn, S. W., & Johnson, W. C., Jr. (1992) *Anal. Biochem. 200*, 321−331.
van Snick, J. (1990) *Annu. Rev. Immunol. 8*, 253−279.
Vriend, G. (1990) *J. Mol. Graph. 8*, 52−56.
Ward, L. D., Zhang, J.-G., Checkley, G., Preston, B., & Simpson, R. J. (1993) *Protein Sci. 2*, 1291−1300.
Ward, L. D., Matthews, J. M., Zhang, J.-G., & Simpson, R. J. (1995) *Biochemistry 34*, 11652−11659.
Weber, G., & Young, L. B. (1964) *J. Biol. Chem. 239*, 1415−1423.
Wong, K.-P., & Tanford, C. (1973) *J. Biol. Chem. 248*, 8518−8523.
Xie, D., Fox, R., & Freire, E. (1994) *Protein Sci. 3*, 2175−2184.
Yutani, K., Ogasahara, K., & Kuwajima, K. (1992) *J. Mol. Biol. 228*, 347−350.
Zink, T., Ross, A., Luers, K., Cieslar, C., Rudolph, R., & Holak, T. A. (1994) *Biochemistry 33*, 8453−8463.

BI9604587